High Step up DC-DC Converter Fed from Photovoltaic System

Esraa M. Ismail
Electrical Engineering Dept.
Faculty of Engineering,
Almustansiriyah University
Baghdad, Iraq

Isam M. Abdulbaq
Electrical Engineering Dept.
Faculty of Engineering,
Almustansiriyah University
Baghdad,Iraq

Ammar I. Majeed
Electrical Engineering Dept.
Faculty of Engineering,
Almustansiriyah University
Baghdad, Iraq

ABSTRACT
In this paper, a high efficiency, high step up DC-DC converter fed from a single (250W) photovoltaic panel, through a maximum power point tracker (MPPT), is simulated and implemented using simple topology. This is done by duplicating the output voltage of the flyback converter using a series resonant circuit in its transformer secondary during the "ON" period. It will be shown that this topology leads to increase the power capability of the converter as compared with the conventional one. This source designed to prepare a DC bus voltage for a three-phase inverter. Such a source is quite compatible with a 3-phase stand alone or a grid connected solar systems. The adopted simulation program is LTspice (Linear Technology spice). The prototype of a (250W, 600V) results agrees with that of the simulation.

Keywords
Flyback DC-DC Converter, Photovoltaic Panel, MPPT, Microcontroller

1. INTRODUCTION
The environment of the Middle East is very suitable for using renewable energy like the solar energy (PV energy). PV energy is one of the most important renewable energy types and it will become one of the major contributors for electricity generation. For commercial and residential PV application, the distributed PV system architecture is promising because of its higher energy yield, more flexibility in plant design and improved monitoring and diagnostics capabilities [1]. Renewable energy generation systems are gaining an increased interest in recent years as they are proven to be a reliable source of energy generation. Among them, solar PV (Photo-Voltaic) source is playing a significant role in electrical energy requirements of small, isolated power systems and to satisfy energy demand in remote areas [2]. In order to avoid the pollution of the environment, electrical energy must be generated by a three-phase solar power station. This type of converters, modified to maximize the energy harvesting from photovoltaic systems are called power optimizers. In this paper an efficient PV panel fed step up DC to DC converter suitable as a DC voltage source of a 3-phase inverter is designed, simulated and implemented. The principle of operation explained briefly, with a simple comparison between the transformers of the designed converter and the traditional one. The design includes the application of an algorithm of tracking the maximum power point of the PV panel in spite of the changes in ambient condition. For this purpose, maximum power point tracker (MPPT), is interfaced between the PV panel and the load [3]. The experimental result of the implemented convertor will be demonstrated.

2. PRINCIPLE OF OPERATION
In order to generate a 3-phase 220V from one PV panel a DC to DC converter has an ability to produce about 537volts DC at least to feed a three phase inverter as shown in figure (1). The solar panel has a low voltage DC power even at the higher illumination. The I-V characteristic curve of the considered PV panel is shown in figure (2).

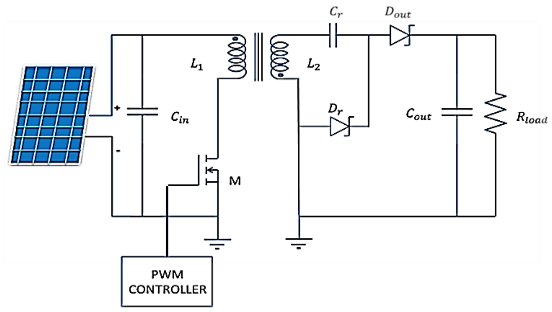

Figure (1): The Circuit Diagram of High Step Up DC-DC Converter [4]

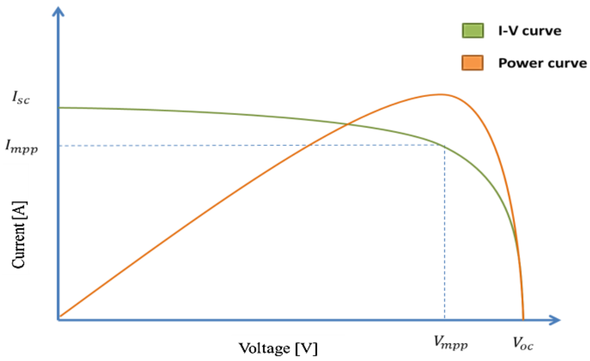

Figure (2): I-V Curve of the Solar Panel

Figure (3) shows the equivalent circuit of the high efficiency, high step-up voltage gain converter. This converter adds one pair of additional capacitor and diode to achieve high step-up voltage gain. In this topology the transformer utilization will be similar to that of a the forward type and the flyback type converter as well. Its capacitor C_r can be charged in parallel and discharged in series via the secondary winding of the transformer. The turns ratio of the transformer $N = (N_2/N_1)$ used to raise the secondary voltage to NV_{pv} volts, where V_{pv} is the terminal voltage of the solar panel across the input capacitor. The transformer secondary circuit composed of a series resonant circuit consists of C_r and the transformer leakage inductance L_k.

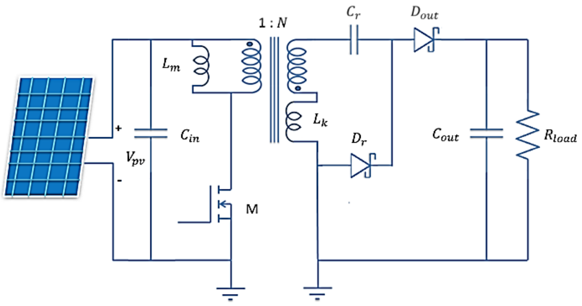

Figure (3): Converter Equivalent Circuit Diagram

To understand the operation of this converter, the three modes of operation must be explained as follows.

First mode $[t_1 - t_2]$: as shown in figure (4-a), during this period M is turned to "on" state and D_r too. A secondary circuit composed of C_r and L_k will resonate and a positive half cycle of a sinusoidal current i_{D_r} flowing through the secondary circuit. At the end of the positive half cycle, D_r turned off at zero current (ZCS condition) to minimize the power losses [4] and the capacitor charges to NV_{pv} volts of the polarity shown in figure (4-b). The magnetizing current i_{L_m} and the switch current i_M are expressed as [4].

$$i_{L_m}(t) = i_{L_m}(t_1) + \frac{V_{pv}}{L_m}(t - t_1) \dots\dots\dots\dots\dots\dots\dots (1)$$

$$i_M(t) = i_{L_m}(t) + N\, i_{D_r}(t) \dots\dots\dots\dots\dots\dots\dots\dots (2)$$

Where $i_{L_m}(t)$ Is the magnetizing current
$i_{L_m}(t_1)$ Is the magnetizing current of the previous cycle = $i_{L_m}(t_4)$
L_m Is a magnetizing inductance
V_{pv} Is the photovoltaic panel input voltage
N Is the turn's ratio of the transformer
i_M Is the switch current
i_{Dr} Is the current through the Shottky diode D_r during resonance.

Second mode $[t_2 - t_3]$: M still in "on" state, but the resonance period is finished so i_{D_r} in the secondary circuit will be zero and the diode D_r will be in the "off" state and the polarity of C_r is reversed w.r.t the first mode, but i_{L_m} will continue until the end of this mode as shown in figure (4-b).

Third mode $[t_3 - t_4]$: M is turned to "off" state and D_{out} turned to "on" state, while D_r still in "off" state as shown in figure (4-c). The voltage across C_{out} will be the summation of two voltages (the secondary voltage and that across C_r). The diode current $i_{D_{out}}$ decreases linearly due to the relation [4]:

$$i_{D_{out}}(t) = \frac{i_{L_m}(t_3)}{N} - \frac{V_d - V_{C_r}}{N^2 L_m + L_k}(t - t_3) \qquad (3)$$

The magnetizing current i_{L_m} and the switch current i_M are expressed as [4]:

$$i_{L_m}(t) = i_M(t) = i_{L_m}(t_3) - \frac{V_d - V_{C_r}}{N L_m}(t - t_3) \qquad (4)$$

Applying voltage-second balance relation to the primary side will result in:

$$\frac{V_d}{V_{pv}} = \frac{N}{(1 - D)} \qquad (5)$$

Where D is the duty cycle ratio of the pulse width modulation. At the end of the period, C_r discharged completely so, it retains its main polarity, as that at t_1, as it shown in figure (4-d).The value of the magnetizing inductance of the transformer depends on the output power and the average primary current I_{pri}. As the maximum power generated at highest illumination is 290 watts for the solar panel used in this research, so design calculations considered the output power to be 285 watts due to the expected losses, and I_{pri} has two components, the magnetizing current i_M (of an average value represented as I_{Lm}) and the reflected output current from the secondary Ni_{D_r} (of an average value represented as NI_d) as shown in figure (5).

$$L_m = \frac{V_{pv} D T_s}{2 I_{L_m}} \qquad (7)$$

$$I_{pri} = I_{L_m} + N I_d \qquad (8)$$

Substitute (8) in (7) to get the main equation design

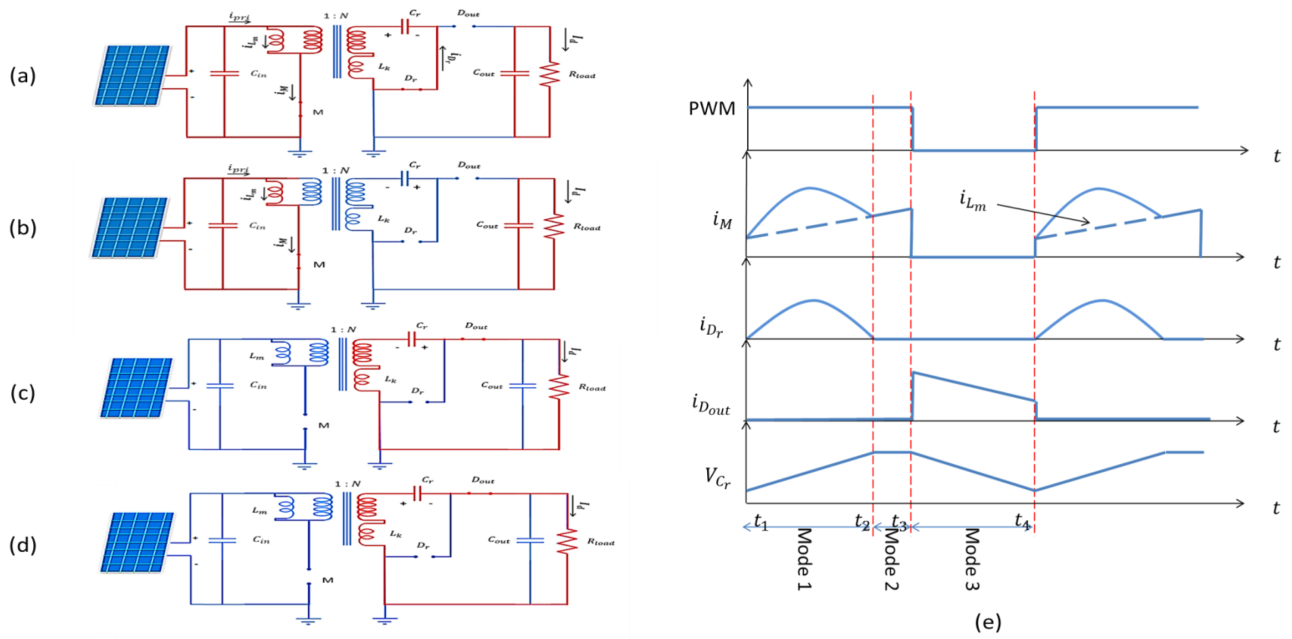

Figure (4): (a) first mode of operation $(t_1 - t_2)$ (b) second mode of operation $(t_2 - t_3)$ (c) third mode operation $(t_3 - t_4)$(d) the polarity of C_r at the end of the cycle is as that at [t_1] (e) waveforms of different operation modes

$$L_m = \frac{V_{pv} D T_s}{2(I_{pri} - N I_d)} \quad (9)$$

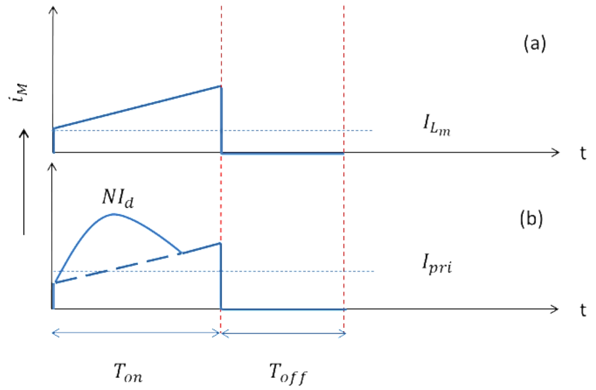

Figure (5): primary current components (a) magnetizing current (b) summation of magnetizing and reflected output currents

To ensure zero current switching ZCS occur then ω_r must be higher than ω_s .

$$\omega_r = \frac{1}{\sqrt{L_k\, C_r}} \quad (10)$$

Where ω_r is the angular resonant frequency [4], and the ω_s is the angular switching frequency. Figure (4-e) illustrates the waveforms for the PWM, i_{Dr} , $i_{D_{out}}$, i_M and V_{C_r}.

3. MAXIMUM POWER POINT TRACKER or MPPT

3.1 An Overview

A MPPT or maximum power point tracker is a strategy followed to harvest the most generated power from such a sources like PV systems and wind turbine or other systems. And in this research there is an electronic DC to DC converter that matches between the solar array (PV panels), and the resistive load. To put it simply, they convert a high voltage DC output from solar panels up/down to the voltage needed to such a wide application. You cannot dispense it in any way if you are using solar panels. There is some confusion about the term "sun tracking" or Panel tracking this is where the panels are on a mount that follows the sun. These optimize output by following the sun across the sky for maximum sunlight. These typically give you about a 15% increase in winter and up to a 35% increase in summer. This is common in regions have shorter days, but in the Middle East region at most days in the year have long daylight and using sun tracker not get a real difference in the output of the panel. And that's not like an MPPT controller work. The MPPT has many topologies that proportional to the output voltage, efficiency of the converter and the cost. Figure (6) shows the characteristic power curve for a PV array. The problem considered by MPPT techniques is to automatically find the voltage V_{MPP} or current I_{MPP} at which a PV array should operate to obtain the maximum power output P_{MPP} under a given temperature and irradiance. It is noted that under partial shading conditions, in some cases it is possible to have multiple local maxima, but overall there is still only one true MPP. Most techniques respond to changes in both irradiance and temperature, but some are more specifically useful if temperature is approximately constant. Most techniques would automatically respond to changes in the array due to aging, though some are open-loop and would require periodic fine-tuning. In our context, the PV array will typically be connected to a power converter that can vary the current coming from the PV array [5]. To reach the optimum converter and MPPT controller design must have much information about your PV panel. Table (1) illustrates the parameters of SOLAR ONE 250W PV panel.

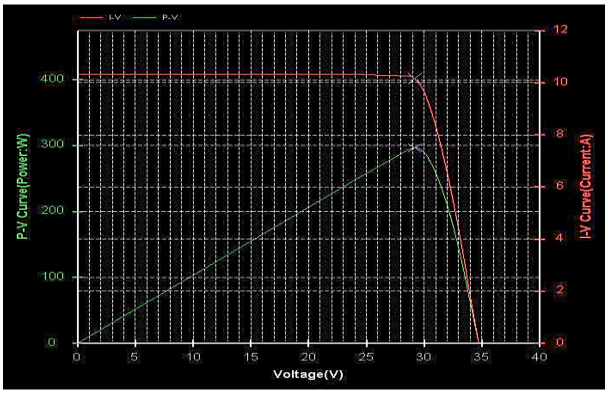

Figure (6): PV panel characteristics used in this research

Table 1: Parameters of the PV panel SOLAR ONE 250W tested by "Sun Simulator"[6]

Operator	value
Product ID	0000000000000011
Current temperature coefficient (mA/℃)	2.0000
Voltage temperature coefficient (mV/℃)	-2.0000
Model area (cm2)	100.00
Sensor temperature (℃)	32.5
Irradiance (mW/cm2)	100.0
Isc (A)	10.3186
Voc (V)	34.7315
PMPP (W)	296.4684
IMPP (A)	10.1569
VMPP (V)	29.1889
F.F. (%)	82.72
Module efficiency (%)	29.6541
Estimated shunt resistance (ohm)	180.5127
Estimated series resistance (ohm)	0.1401

As the power supplied by the solar array depends on the insolation, temperature and array voltage, an important consideration in the design of an efficient solar array system is to track the maximum power point correctly. The purpose of the MPPT is to move the array operating voltage close to the MPP under changing atmospheric conditions [7]. Most of the design guides are based on the constant output while the input can have some pulsation of voltage. The difficulty of the MPPT design is that the input voltage and output voltage are variable [8]. The methods of MPPT vary in complexity, sensors required, convergence speed, cost, range of effectiveness, hardware implementation, popularity, and in other respects [5].

3.2 Microcontroller PIC

The microcontrollers played revolutionary role in the embedded industry after the invention of Intel 8051. The steady and progressive research in this field gave the industry more efficient, high-performance and low-power consumption microcontrollers. The AVR, PIC and ARM are the prime examples. The new age microcontrollers are getting smarter and richer by including latest communication protocols like USB, I2C, SPI, Ethernet, CAN etc. [9].

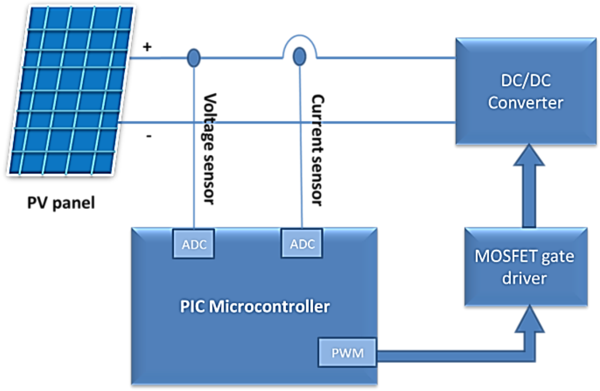

Figure (7): microcontroller block diagram

The PIC microcontroller is very easy to use. It is a single chip can do all functions you need like ADC (analog to digital converter), timer, comparator, PWM generator and all mathematical functions. In this paper PIC get two values in analog form from the sensors in the figure (7) and convert it to digital form by ADC function, then multiplied it to get the power coming from the PV panel P_{pv} and compare whether this power more the old one P_{pv_old}. From that condition it can decide to increase or decrease the duty cycle ratio. Figure (8) shows the control algorithm.

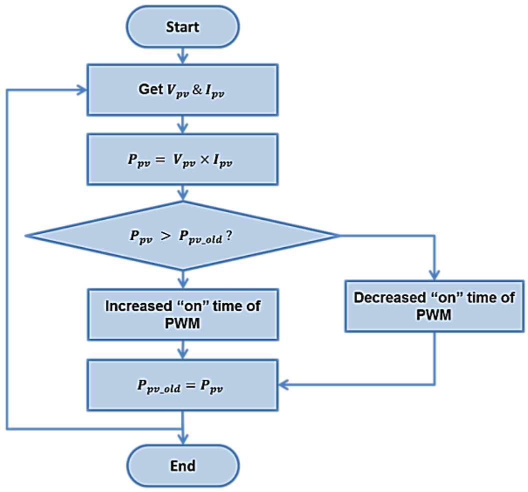

Figure (8): the control algorithm

4. SIMULATION AND EXPREMANTAL RESULT

In reference [4] the DC-DC converter prototype designed to drive 180W and 380V output, while this converter designed to drive 285W and 560V output. The input voltage of the converter is the photovoltaic panel voltage V_{pv} (maximum power point voltage V_{mpp}). When the switch M turn "on" the primary inductance, voltage V_L will be equal to V_{pv} and C_r voltage V_{C_r} will be equal to NV_{pv}. The additional resonant circuit (C_r and D_r) uses to reduplicate the secondary voltage, so the gain of the converter will be twice the conventional converter (flyback converter) if the duty cycle is 50%. And therefore the converter will be able to transfer more as compared with the conventional one for the same parameters of the transformer used in it. Those converters are used as a fast primary switch. The fast turn on and turn off behavior of the primary switch produces a high (dv/dt). This fast voltage transition produces an overshoot and lead to ringing waveforms when the switch turns off. That must be properly suppressed. Without this, semiconductors can fail and conducted and radiated noise levels will be higher than necessary. The high frequency ringing must be damped using RC or RCD snubber networks. On the primary side a possible location for the RC network across the transformer primary terminals. The more effective the RC network is, the more power is dissipated in the resistor. This can lead to lower standby efficiency, which could be a problem with renewable energy power supplies. Note figure (9).

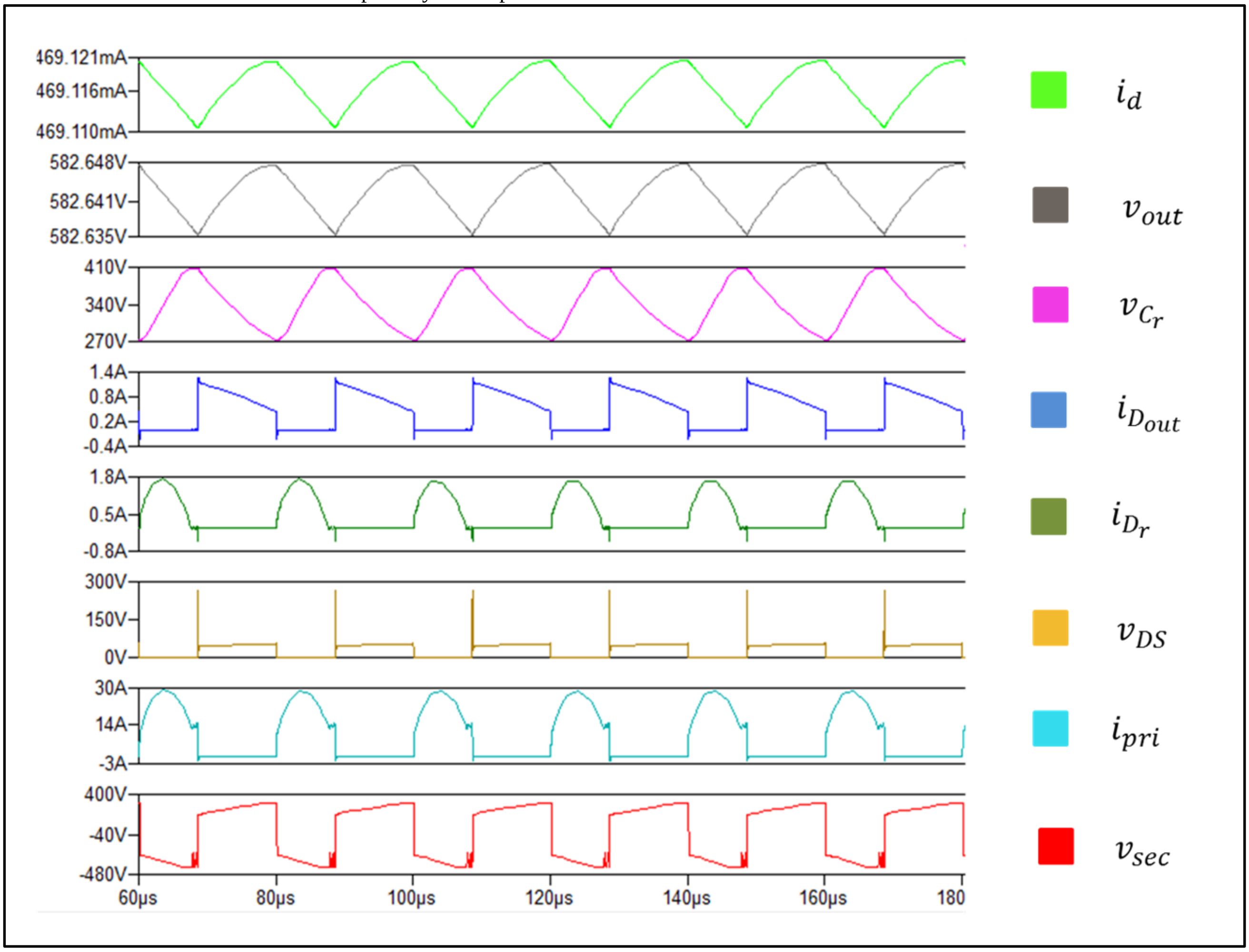

Figure (9): Proposed Converter LTspice Simulator Waveforms

The simulation result makes sure that the power can be drive in more than 94.66% efficiency without any problem. The transformer has been built on reality and tested to measure its leakage inductance to be similar to that in the simulation program to get the same result. The model has been built practically in the laboratory as shown in picture (1).

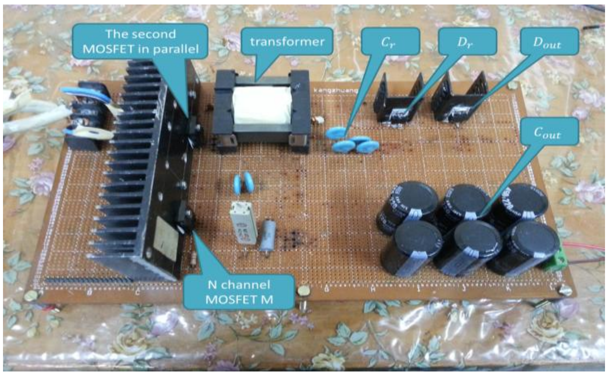

Picture (1): the proposed converter implemented in the laboratory

The primary current reaches 9.8 Amperes, and that cause an excessive heat in the MOSFET. To decrease the heating, two MOSFETs are connected in parallel to decrease the on state resistance of the MOSFET to a half of its value and increase the efficiency practically.

The MOSFET gate driver circuit delivered the MOSFET gate pulsating voltage with maximum voltage 12 volt and duty cycle ratio of 42% as shown in figure (10) the pictures get it by using RIGOL DS1102E DIGITAL OSCILOSCOPE. The MOSFET driver chip used in the MOSFET gate drive circuit is MC34151P.

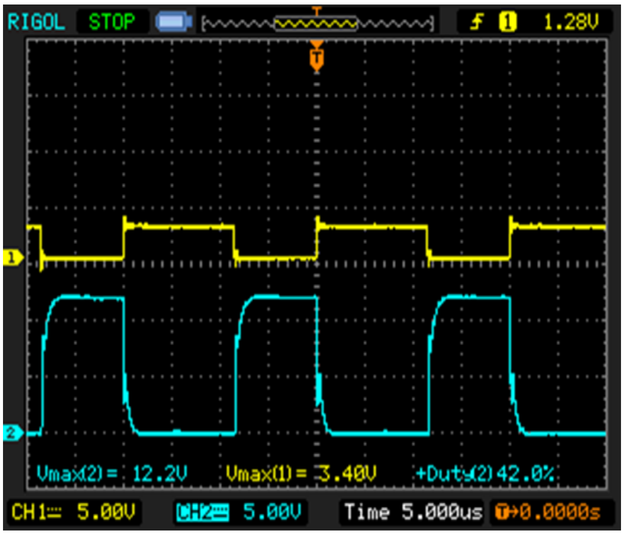

Figure (10): MOSFET gate driver waveforms (CH1) V_{pulses} MOSFET gate driver voltage waveform and (CH2) V_{logic} output digital PWM waveform from PIC

The switch M breakdown voltage must be chosen to be three times the drain to source voltage V_{DS} to avoid failing during the operation. V_{DS} Is the sum of the reflected voltage V_{ref} and the input voltage V_{pv} . V_{ref} is the secondary winding voltage at the off time.

$$V_{ref} = V_{out} - V_{C_r} \quad (10)$$

$$V_{DS} = \frac{V_{ref}}{N} + V_{pv} \quad (11)$$

Figure (11) shows V_{DS} waveform with the sharp spikes appears at the beginning of the off time. In the conventional flyback converter, the voltage gain can be easily achieved by increase the turns-ratio of transformers, but this will leads to induces high voltage stress and switching losses [10] due to the leakage energy.

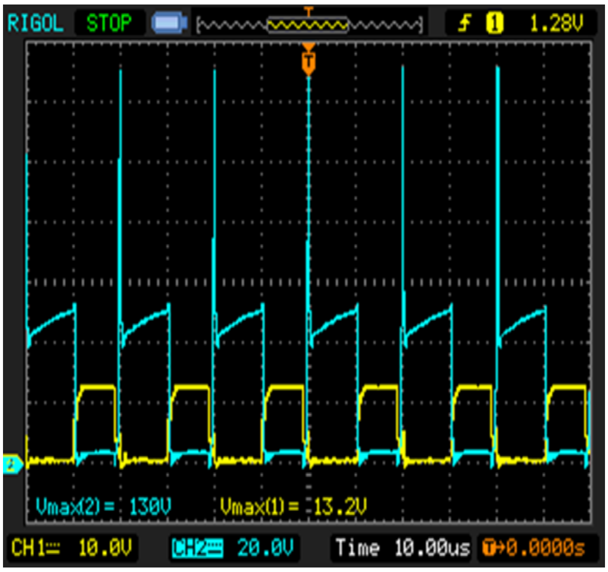

Figure (11): M switch waveforms (CH1) V_{pulses} MOSFET gate drive voltage waveform and (CH2) V_{DS} drain source voltage waveform

The series resonant circuit current of frequency 62.5 kHz is shown in figure (12).

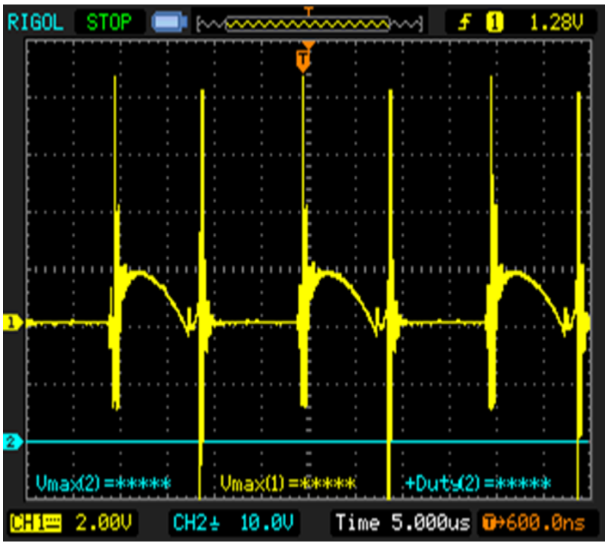

Figure (12): (CH1) series resonant circuit current waveform (CH2) grounded

The output DC voltage appearing in figure (13) below.

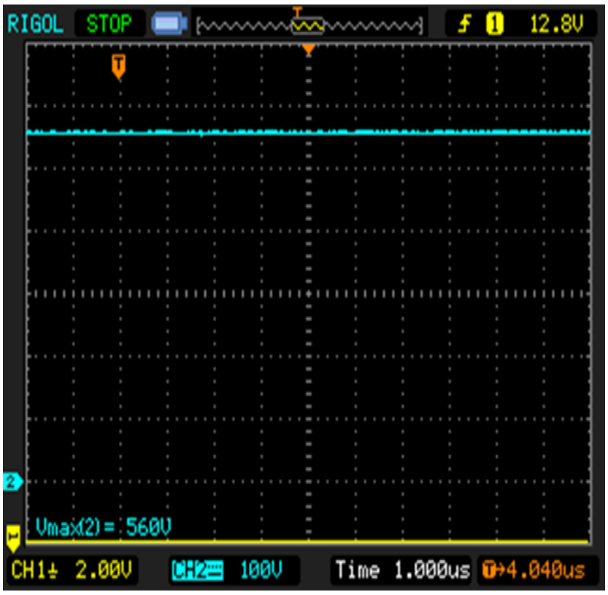

Figure (13): (CH2) output voltage waveform (CH2) grounded

5. TRANSFORMER

The transformer used in this (290W) converter is suitable for the conventional flyback converter of (60W) only. Hence, this will reduce the stress on the components due to the transformer leakage reactance and the cost. The leakage inductor of the transformer incurs a voltage spike on the main switch and affects the conversion efficiency [11]. Flyback power supplies use the least number of components. At power levels below 75 watts, total flyback component cost is lower when compared to other techniques. Between 75 and 100 Watts, increasing the voltage and current stresses cause flyback component cost to increase significantly [12]. While in proposed converter find the cost not increase significantly when adding another diode and capacitor, but achieve high power, low switch stresses and high gain. Table (2) illustrates the difference in power driving for the same transformer in the two different topologies. The figures (9) and (14-a) illustrate the comparison between waveforms for each converter, then notes figure (4-e) and figure (14-b).

Table (2): comparison between proposed converter and conventional flyback converter for the same transformer

System parameter	Proposed converter	Conventional flyback
V_{pv}	29V	29V
V_{out}	560V	252V
P_{mp}	290W	60W
D	0.42	0.42
f_s	50kHz	50kHz
L_m	28uH	28uH
L_k	0.65uH	0.65uH
C_r	10uF	---
C_{out}	330uF	1uF
N	12	12
R_{load}	1240Ω	1058Ω

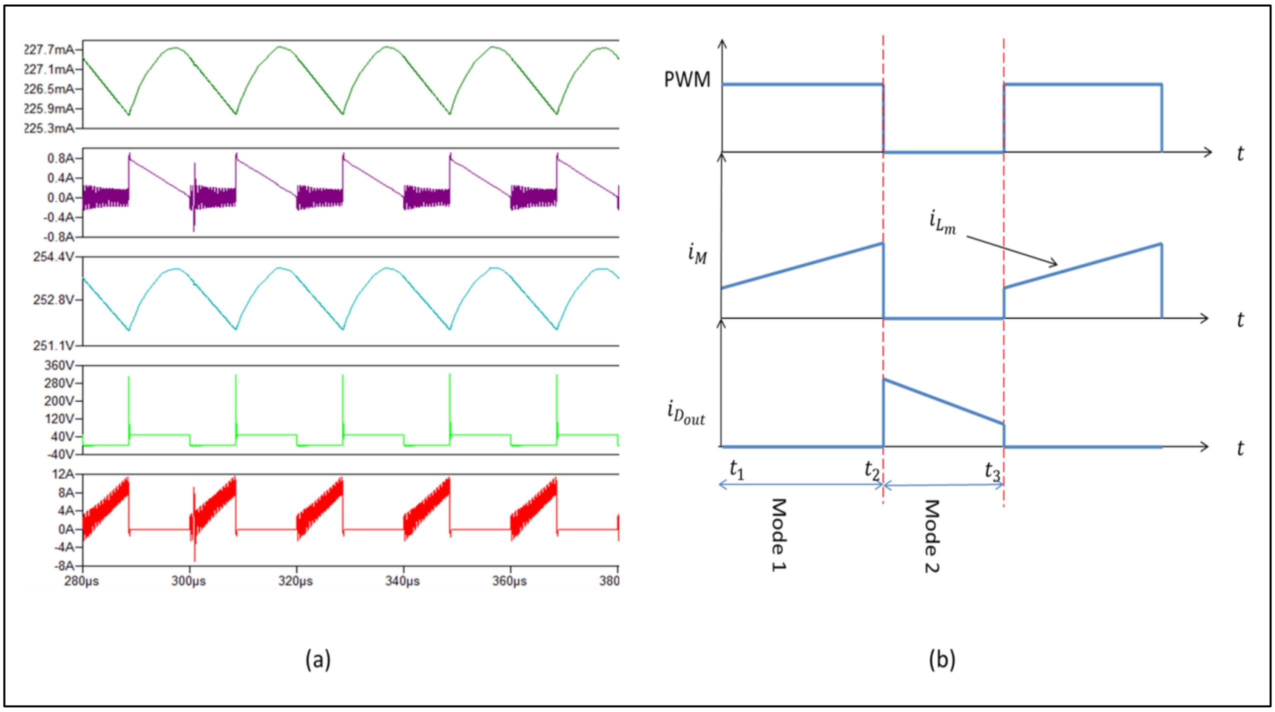

Figure (14): (a) conventional flyback converter LTspice simulator performance waveforms (b) conventional flyback converter modes

6. CONCLUSION

The previous analysis of the proposed converter, it is clear that this converter is very flexible to be used as a PV fed DC power supply suitable for a stand-alone 1-phase or 3-phase inverter as well as it can be used for a grid connected system. Also, it can be used to overcome the shading problem in a wide field of PV panels, if the DC output of each panel can be connected to a common DC bus, then they can be considered as a parallel connected DC sources feeding a single 3-phase inverter. It is simple, cheap, and efficient high voltage DC converter due to its small ferrite transformer as compared to a conventional one.

7. REFERENCES

[1] Zhigang Liang, Alex Q. Huang, Rong Guo "High Efficiency Switched Capacitor Buck-Boost Converter for PV Application", IEEE, p.p (1951-1958), 2012.

[2] Neha Adhikari, Bhim Singh, A. L. Vyas, Ambrish ChandraKamal-AI-Haddad, "Analysis and Design of Isolated Solar-PV Energy Generating System", IEEE, 2011.

[3] Abu Tariq *and* M.S. Jamil Asghar, "Development of Microcontroller-Based Maximum Power Point Tracker for a Photovoltaic Panel", IEEE, 2006.

[4] Woo-Young Choi*, Change-Goo Lee, "Photovoltaic panel integrated power conditioning system using a high efficiency step-up DC-DC converter", Elsevier, Renewable Energy, p.p (227-234), 2011.

[5] Trishan Esram, and Patrick L. Chapman, "Comparison of Photovoltaic Array Maximum Power Point Tracking Techniques", IEEE transactions on energy conversion, p.p (439-448), 2007.

[6] Ministry of Industry and Minerals, Corporation of Research and Industry Development, Energy and Environment Research Center (EERC).

[7] Chihchiang Hua and Chihming Shen "Study of Maximum Power Tracking Techniques and Control of DC/DC Converters for Photovoltaic Power System", IEEE, p.p (86-93), 1998.

[8] Pavels Suskis,Ilya Galken, Janis Zakis, "Design and Implementation of Flyback MPPT Converter for PV-Applications", IEEE, p.p (291-296), 2014.

[9] Nikhil Agnihotri "http://www.engineersgarage.com/articles/pic-microcontroller-tutorial".

[10] A. TOMASZUK_ and A. KRUPA, "High efficiency high step-up DC/DC converters – a review", BULLETIN OF THE POLISH ACADEMY OF SCIENCES TECHNICAL SCIENCES, power electronics, p.p (475-483), 2011.

[11] Yi-Ping Hsieh, Jiann-Fuh Chen, Tsorng-Juu Liang, Lung-Sheng Yang, "A Novel High Step-Up DC-DC Converter for Microgrid System", IEEE Transaction on Power Electronics, 2010.

[12] Power Integrations, "Flyback Transformer Design for TopSwitch Power Supplies", Application Note AN-17, PowerInt., 1994.